EXPERIMENTAL AND KINETIC STUDY OF THE INTERACTION OF A COMMERCIAL SOOT TOWARD NO AT HIGH TEMPERATURE

C. Arnal, M.U. Alzueta, A. Millera and R. Bilbao
amillera@unizar.es
Aragón Institute of Engineering Research (I3A), University of Zaragoza. Campus Río Ebro.
C/ Andador Mariano Esquillor s/n, 50018 Zaragoza, Spain. Phone: +34976761876, Fax: +34976761879

Abstract
An experimental and kinetic study at high temperature was made of the interaction of NO with Printex-U, a commercial carbon black, considered as diesel soot model compound. Foremost, a characterization of this soot was performed by using different techniques like: elemental analysis, BET surface area analysis, SEM, TEM and XRD. Two series of experiments were carried out. The first one took into account the inlet NO concentration influence (from 200 to 2000 ppm) at a given temperature of 1273 K. In the second one, the temperature influence (from 1173 to 1373 K) at a given NO concentration of 2000 ppm was considered. From the experimental results, a strong effect of the inlet NO concentration and temperature was observed. A kinetic model, the Shrinking Core Model with decreasing size particle and chemical reaction control, was successfully applied, obtaining a fractional reaction order of 0.26 and an activation energy of 110 kJ/mol.

1. Introduction

The increase of diesel vehicles in the recent past years may be explained because diesel engines reach high fuel-efficiency and durability compared with gasoline ones. Besides, for diesel vehicles the fuel consumption is lower, and thus, they release less carbon dioxide (main gas responsible for global warming). However, in diesel engine exhaust, particulate matter (also known as soot) and nitrogen oxides (NO_x) are present as main pollutants, which health effects on human and environment problems are of great concern and also well known [1-4]. Soot and NO_x emissions from diesel engines are mainly conditioned by the competition of the reactions that take part in their formation and elimination [2]. These compounds may react *in situ* with each other and reduce, thus, their emissions at the same time [5,6]. Therefore, this reaction may be considered as a strategy of elimination of these air pollutants at the same time.

The reaction of NO with different carbonaceous materials has been studied earlier [1,4,6,7]. In these studies, in general, CO, CO_2 and N_2 have been considered the main gas products of the reaction. This process can be expressed globally through the following reactions [8]:

$$C + NO \rightarrow CO + \tfrac{1}{2} N_2 \quad \text{(R.1)}$$

$$C + 2NO \rightarrow CO_2 + N_2 \quad \text{(R.2)}$$

$$CO + NO \rightarrow CO_2 + \tfrac{1}{2} N_2 \quad \text{(R.3)}$$

As it may be observed, NO is reduced to nitrogen and the carbon products are carbon monoxide and carbon dioxide. Reaction R.3, according to Li et al. [8], is a catalytic reaction catalyzed by the carbon-surface and enhanced in CO presence. Therefore, this reaction will be significant when CO concentration is high.

The carbon-NO reaction can be mainly affected by temperature, NO concentration and the characteristics of the carbonaceous materials [8]. Furthermore, different kinetic models have been employed in carbon-NO reaction analysis. According to this, several studies for different kinds of carbonaceous materials have proposed different reaction orders and activation energy values (see Table 1). Table 1 summarizes the reaction orders and activation energy values obtained with respect to NO by several authors, pointing out the reactor and temperatures used and the carbonaceous material utilized as well as their surface area characterized by N_2 adsorption isotherms (77 K) by using the BET equation.

Table 1. Reaction order, activation energy with respect to NO for carbonaceous material-NO reaction and BET surface area.

Carbon type	Reactor	Temperature range (K)	NO pressure (kPa)	Activation energy ($kJ \cdot mol^{-1}$)		Reaction order	Surface area (m^2/g)	Reference
				Low temp.	High temp.			
Phenol-formaldehyde resin char	T.G.A.	773-1073	1.0-10.1	63-88	180	1	100-200[a]	9
Graphite	Fixed bed	873-1173	0.04-0.91	-	239	1	3.7	10
Lignite char	Fixed bed	723-1173	0.05-1.01	-	183	1	402-555 [a]	10
Phenol-formaldehyde resin char 2	T.G.A.	723-1173	1.0-8.1	40	135	1	14-211	11
Phenol-formaldehyde resin char 2	Fixed bed	873-1073	0.001-0.03	27	168	0,77	14-167	11
Graphite	T.G.A.	873-1223	1.0-8.1	65	200	1	17-100	11
Graphite	Fixed bed	873-1223	0.001-0.03	19	245	0,95	5-10	11
Subbituminous coal	Fixed bed	973-1173	0.062-0.308	111		0,22	257	12
Lignite coal	Fixed bed	850-1123	0.062-0.308	116		0.23	20	12
Eucalyptus char LHR [b]	Fixed bed	1023-1173	0.03-0.11	160		0.61	362 [a]	5
Eucalyptus char HHR [c]	Fixed bed	1023-1173	0.03-0.11	130		0.81	539 [a]	5
Soot A: from the pyrolysis of 50000 ppm of acetylene	Fixed bed	1373	0.18-0.22	-		0,5	13.1	6
Soot B: from the pyrolysis of 5000 ppm of acetylene	Fixed bed	1373	0.03-0.22	-		0,7	30.2	6

[a] Surface area determined with CO_2 (273 K); [b] Low Heating Rate of pyrolysis; [c] High Heating Rate of pyrolysis.

Although significant research has been performed in the interaction of different carbonaceous materials with NO, the reactivity of soot with NO has hardly been studied at high temperatures, relevant to in-cylinder conditions where the work temperature ranges from 900 to 2100 K, approximately [13]. In this context, it is of interest to analyze the process of soot-NO interaction at high temperatures. One commercial surrogate for soot, called Printex-U, was found in literature [3,14,15] to be a representative model compound for diesel soot. The origin of the Printex-U carbon black is the result of thermal-oxidative decomposition process called Degussa Gas Black of a mineral oil [16]. Therefore, the objective of this study is to evaluate the reactivity of the commercial surrogate for soot, Printex-U, toward nitrogen monoxide considering both temperature and inlet NO concentration in order to analyze these influences as well as being able to obtain the kinetic parameters of this process.

2. Experimental Section and Methodology

The experiments were carried out in an experimental installation that consists of a gas feeding system, a reaction system and a system of gas analysis, which has been previously described and used with success [6,17].

Gases are fed and dosed through mass flow controllers. The reacting gas is constituted by nitrogen monoxide in nitrogen, and the gas used to complete the balance to reach a total flow rate of 1000 mL/min (STP) is N_2. The reaction takes place within a quartz tubular reactor which includes a bottleneck in the middle, where a quartz wool plug is placed. Soot is mixed with silica sand particles in a soot/sand ratio of 1/30 (wt.) to facilitate the introduction of the soot sample into the reactor and to prevent soot particle agglomeration. This mixture is deposited over the plug, resulting in a thin layer. The quantity of soot placed into the reactor is, for every experiment, around 10 mg. The sample is heated up from room temperature to the reaction temperature at 10 K per minute in an inert atmosphere of nitrogen. The temperature of bed is measured by a thermocouple located just under the quartz wool plug. Once the desired temperature is reached, a fraction of the nitrogen is replaced by the reactant gas which is fed into the reactor. A systematic working procedure was established to assure the experimental results to be repetitive.

The experiments carried out in this work are presented in Table 2 and include the study of the inlet NO concentration influence (from 200 to 2000 ppm) at a given temperature of 1273 K and the study of the temperature influence (from 1173 to 1373 K) at a given NO concentration of 2000 ppm.

Table 2. Experimental matrix for Printex-U experiments with NO.

Experiments	NO concentration (ppm)	Temperature (K)
1	200	1273
2	500	1273
3	1000	1273
4	1500	1273
5	2000	1273
6	2000	1173
7	2000	1223
8	2000	1273
9	2000	1323
10	2000	1373

Product gases, mainly NO, CO and CO_2, are cooled down to room temperature, go through a particulate matter filter and, eventually, are measured using a continuous infrared (IR) gas analyzer for NO and another one for CO and CO_2. The outlet gas composition is recorded every 10 or 15 seconds.

In the analysis of the experimental results, the NO conversion is defined as:

$$X_{NO} = \frac{C_{NO,i} - C_{NO,o}}{C_{NO,i}} \tag{1}$$

where $C_{NO,i}$ and $C_{NO,o}$ are the inlet and outlet NO concentrations, respectively for different reaction times [18].

In these experiments of soot interaction with nitrogen monoxide, carbon is mainly converted into CO and CO_2 as reaction products, as mentioned before. The carbon weight remaining within the reactor at any time (W_C) is calculated from the measured time variation

of CO and CO_2 concentrations (C_{CO} and C_{CO2}, respectively), in ppm, of the outlet gas. In this way, the initial amount of carbon (in mg) in the reactor (W_{C0}) was determined as:

$$W_{C_0} = M_C \cdot F_t \cdot 10^{-3} \int_0^{\infty} \left(C_{CO} + C_{CO_2} \right) dt \tag{2}$$

M_C is the atomic weight of carbon and F_T is the outing flow expressed in mol per unit time and is expressed by Equation 3:

$$F_t = \frac{Q \cdot P}{R_g \cdot T} \tag{3}$$

where Q is the feeding flow rate, P represents the reactor pressure, R_g is the universal gas constant in appropriate units, and T is the reactor temperature. Hence, the weight of carbon remaining in the reaction at a given time may be calculated as:

$$W_C = W_{C_0} - M_C \cdot F_t \cdot 10^{-3} \int_0^{t} \left(C_{CO} + C_{CO_2} \right) dt \tag{4}$$

The carbon conversion at any time, X_C, may be calculated from Equation 5:

$$X_C = \frac{W_{C_0} - W_C}{W_{C_0}} \tag{5}$$

The characterization of Printex-U has been carried out by using different techniques such as: elemental analysis, Brunauer Emmet Teller (BET) surface area analysis, Scanning Electron Microscopy (SEM), Transmission Electron Microscopy (TEM) and X-Ray Diffraction (XRD), which have been chosen due to their demonstrated suitability for carbonaceous materials.

3. Results and Discussion

The objective of this work is to analyze the influence of temperature and the inlet NO concentration on soot-NO interaction. It is well established that heterogeneous reactions between soot and different gases, generally present in combustion atmospheres (like NO), are affected by soot properties. Therefore, foremost, the characterization of this commercial soot has been performed by using the techniques above mentioned.

3.1 Characterization

In this section, selected results obtained from the characterization of Printex-U will be shown.

Table 3 shows the elemental analysis, ash content, as well as C/H ratio, in molar basis, of Printex-U. The results obtained are very similar to the results showed by Jung et al. [3] for the same material. It was obtained that Printex-U is mainly composed by carbon. Hydrogen, nitrogen, sulphur and oxygen are also present but in smaller quantities. Hydrogen and oxygen may act as adsorption sites, thus could be related to the availability of active sites in soot and, therefore, could influence its reactivity with the different gases present in combustion systems [19]. Hence, high hydrogen content and, therefore, a low C/H ratio value, are related to higher available active sites and to a higher reactivity of the material and Printex-U has a low C/H

ratio value (Table 3) as compared to other soot samples [20]. Ash content [16] is also presented in Table 3. It can be noticed that the ash content may be considered as negligible.

Table 3. Elemental analysis and ash content of Printex-U.

	C	H	N	S	O	C/H (moles)	Ash content (% wt.)
% (wt.)	95.56	0.92	0.32	0.27	3.71	8.56	0.02

The surface area of soot is a critical parameter since it can strongly influence the soot reactivity. In this study, the macro and mesoporous area has been determined by N_2 adsorption at 77 K using BET equation. BET surface area was 92.46 m^2/g. In general, the higher surface area value, the more available active sites there are, what is directly related to higher reactivities. This value is not as high as the ones found for other carbonaceous materials as coal and biomass chars (see Table 1) but it is high compared to other soot samples [20,21].

By means of X-Ray Diffraction, the structural characteristics of soot can be examined (Figure 1). The peak around $2\theta = 25^o$ corresponds to (002) reflection of carbon due to the stacking structure of graphitic basal planes. The background intensity is caused by the amorphous carbon concentration in the soot and the apparent asymmetry of the (002) band is due to the existence of the γ band on its left-hand side, at around 20^o, which is associated with the packing of saturated structures such as the aliphatic side chains grafted on the edges of soot crystallites. On the other hand, it is observed at $2\theta = 44^o$ the two-dimensional band (10), which is attributed to graphite-like atomic order, within a single plane. Based on the analysis of Printex-U, it can be concluded that this sample compared with chars obtained from rice husk and eucalyptus [19], has less amorphous structure and less aliphatic side chains in comparison to the chars, as reflected by the higher background intensity and (002) band asymmetry of the latter. Moreover, the peak (10) is less sharp for Printex-U, indicating a lower crystallite diameter in this solid. These results reveal that soot structure is more ordered compared to chars.

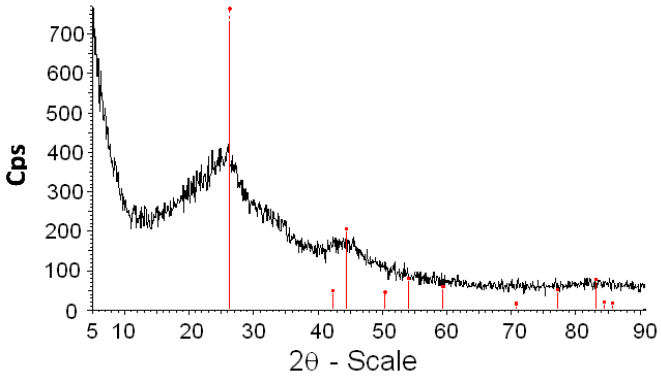

Figure 1. X-Ray Diffraction pattern of Printex-U sample.

Microscopy techniques were used in this study to analyze the structure and morphology of soot sample: shape, size, distribution of the particles and layer orientation. SEM is helpful to analyze the macrostructure and morphology of soot. Figure 2a shows a SEM image from Printex-U in which joined small and spherical particles to create particle aggregates of different sizes may be found. TEM images allow analyzing the nanostructure of sample. Large parallel graphitic layers may be observed for Printex-U in Figure 2b, parallel to each other and proximately parallel to the particle perimeter, as well as the onion-like layers and

the chain-like structure (Figure 2c) of the soot particles. Moreover, several diameter sizes may be observed. They range from 30 to 45 nm.

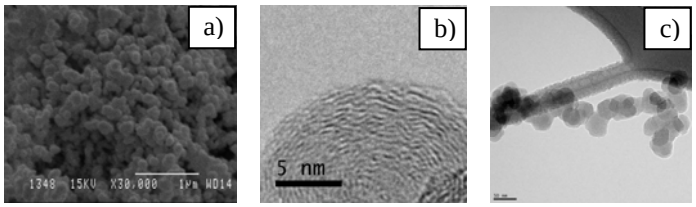

Figure 2. Pictures obtained from microscopic techniques for Printex-U: a) SEM image, b) TEM image c) TEM image.

3.2 Experimental results

Inlet NO concentration and temperature are important variables in the interaction of NO and the carbonaceous materials [1]. Below, the influence of these operating conditions as well as the concentrations of the main gas products will be analyzed.

The importance of the carbonaceous solids properties on the formation of the main gas products in the reaction of the different carbonaceous materials with NO has been studied by several authors. Yang et al. [22] studied the interaction of NO with four carbonaceous materials: natural graphite, carbon black, activated carbon and fullerene black, where CO and CO_2 were the main carbon-gas products. From their work, they concluded that the reaction of NO with natural graphite and carbon black had a higher selectivity to CO than the reaction of NO with activated carbon and fullerene black. The carbonaceous material employed in this work is a carbon black and the situation explained by Yang et al. [22] is what occurs in the present study. CO is the main carbon-product obtained in the interaction soot-NO while CO_2 concentrations are never over 20-30 ppm.

Following, the experimental results are analyzed and shown. The range of the inlet NO concentration of 200-2000 ppm was chosen because NO_x concentrations present in diesel exhaust gases, hence formed within the cylinder, are between 100 to 600 ppm, mainly as NO [4]. Higher concentrations than 600 ppm of NO were selected so that the reaction soot-NO was not too slow. Figure 3a shows the influence of the inlet NO concentration on the evolution of carbon conversion as function of time, while Figure 3b illustrates NO conversion determined by Equation 1.

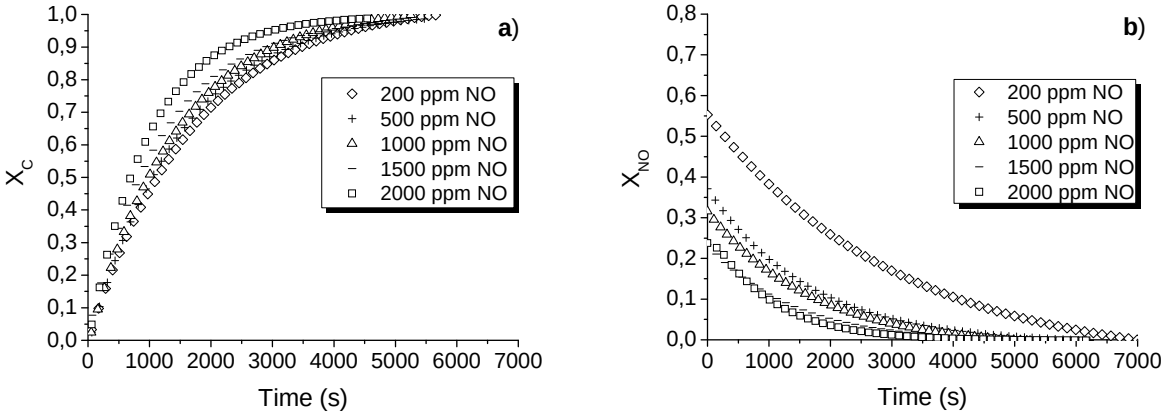

Figure 3. Evolution of: a) carbon conversion and b) NO conversion as function of time. Influence of inlet NO concentration at 1273 K.

According to Figure 3, it is clear that inlet NO concentration affects the carbon consumption in the interaction soot-NO, affecting directly to carbon conversion, being higher

when increasing inlet NO concentration. It also impinges on NO conversion, being higher when NO concentration decreases. The NO conversion dependence on the inlet NO concentration is in agreement with Sørensen et al. [23] who used wheat straw char.

Temperature is the other key operating parameter taken into account. The temperature range of 1173-1373 K was selected because at diesel-engine like conditions these temperatures are reached [13]. Figure 4 shows carbon conversion (Figure 4a) and NO conversion (Figure 4b) evolution as function of time for different temperatures.

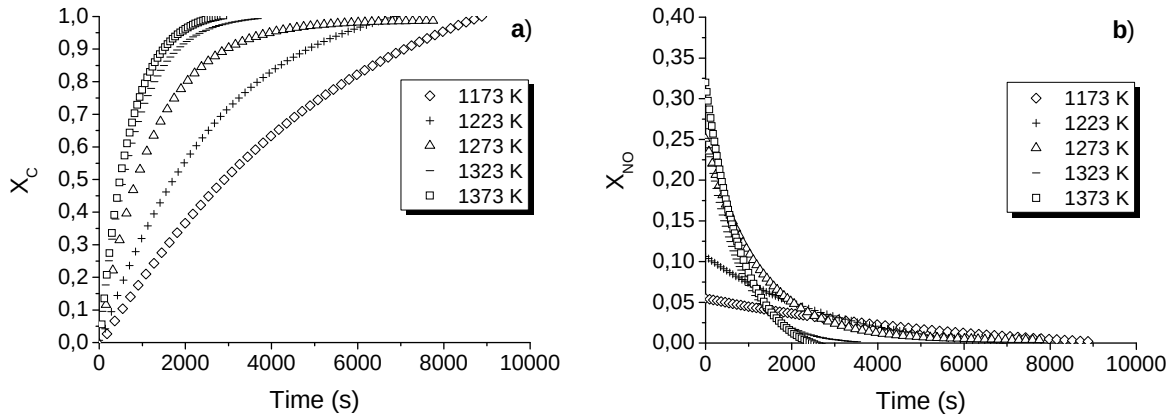

Figure 4. Evolution of: a) carbon conversion and b) NO conversion as function of time. Influence of temperature with 2000 ppm of NO.

From Figure 4, it can be observed that temperature also influences carbon and NO conversion. In Figure 4a may be noticed that the more temperature, the more carbon conversion which trend is similar to NO conversion, Figure 4b, where the more temperature, the more initial NO conversion is obtained, as Dong et al. [19] found for different carbonaceous materials (sawdust, rice husk and corn straw char).

It is interesting to mention that significant NO reductions can be found. In Figure 3b, NO conversion reaches a value of 0.55 for an inlet NO concentration of 200 ppm at 1273 K and a value of 0.32 is obtained with an inlet NO concentration of 2000 ppm at 1373 K, Figure 4b.

3.3 Kinetics of the carbon consumption with respect to NO

The global process of soot-NO interaction has been considered to be adequately represented by the following stoichiometric equation (R.4) [6]:

$$NO(g) + bC(s) \rightarrow cCO(g) + dCO_2(g) + eN_2(g) \qquad (R.4)$$

where *b*, *c*, *d* and *e* are the stoichiometric coefficients. The coefficient *b* may be calculated from the experimental concentrations of CO and CO_2:

$$b = \frac{\frac{CO}{CO_2} + 1}{\frac{CO}{CO_2} + 2} \qquad (6)$$

The reaction model applied was the Shrinking Core Model (SCM) with decreasing size particle, which is applicable for nonporous materials [24,25]. Since there is no defined BET area limit value which allows differentiating between porous and nonporous materials, the

values given before, in the *Characterization* section, may be considered low enough to be characteristic of nonporous materials. Besides, Printex-U may be considered as an ash-free material (see Table 3). In this reaction model, the kinetic expressions will change depending on the rate-controlling step: the gas film diffusion control or the chemical reaction control. The physical step is usually much less temperature-sensitive than chemical steps [25]. Hence, in order to be able to distinguish between diffusion and chemical reaction control, the experiments carried out at different temperatures were used to determine the controlling step. The results obtained (not shown) pointed out that the chemical reaction was the control step in the interaction soot-NO at the operating conditions described in Table 2. Therefore, the experimental data were processed and the results were treated in agreement with the SCM with decreasing size particle and chemical reaction control equations [24,25]. The carbon consumption rate is expressed as:

$$-\frac{1}{S_{ext}}\cdot\frac{dN_C}{dt} = b\,k_S\,C_{NO}^{n} \tag{7}$$

where the carbon consumption rate is referred to the external surface of the particle, S_{ext}; N_c represents the moles of carbon, k_S is the rate constant of the reaction, C_{NO} is the NO concentration and n is the reaction order with respect to NO.

As Printex-U was considered to be composed by spherical particles, the reaction rate may be expressed as function of the carbon weight remaining within the reactor at any time as follows [6]:

$$-\frac{1}{W_C^{\,2/3}}\cdot\frac{dW_C}{dt} = D\,b\,k_S\,C_{NO}^{n} \tag{8}$$

where D is a constant. The SCM with chemical reaction control has to be applied in the carbon weight interval where the expression ($-1/W_C^{2/3}\cdot dW_C/dt$) is considered as constant. Figure 5 shows the results obtained at 1273 K for different NO concentrations (Figure 5a) and the results obtained with 2000 ppm of NO at different temperatures (Figure 5b). It may be observed that the term just mentioned remains practically constant throughout the experiments and, it is noteworthy to mention that this interval represents more than the 90 per cent of the carbon conversion.

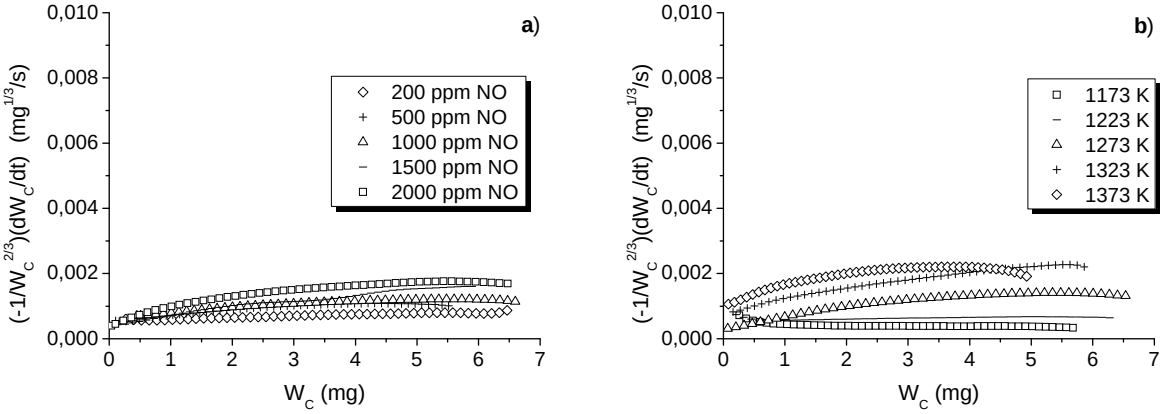

Figure 5. Evolution of carbon consumption rate referred to external particle surface versus remaining carbon weight in the reaction of Printex-U: a) with different NO concentrations at 1273 K and b) with 2000 ppm of NO at different temperatures.

The application of the SCM with decreasing size particle and chemical reaction control implies the fitting of the experimental data to the following equation, connecting time, *t*, and carbon conversion:

$$\frac{t}{\tau} = 1 - \left(1 - X_C\right)^{1/3} \tag{9}$$

where τ is the time needed for the complete carbon conversion. Table 4 summarizes *b* values from Equation 6 and τ values obtained in the fitting of Equation 9 together with the regression coefficients (R^2) of the experiments presented in Table 2.

Table 4. Values of *b* and τ, for the experiments shown in Table 2, obtained from Equations 6 and 9, respectively.

Experiments	b	τ (s)	R^2
1	0.97	8621	0.9966
2	0.98	6536	0.9886
3	0.97	5917	0.9923
4	0.98	5102	0.9900
5	0.98	4464	0.9852
6	0.88	13344	0.9991
7	0.82	9020	0.9990
8	0.98	4464	0.9852
9	0.95	3493	0.9889
10	0.93	2699	0.9953

According to Szekely et al. [24] and Levenspiel et al. [25], τ is defined as follows:

$$\tau = \frac{\rho_C R_0}{b k_S C_{NO}^n} \tag{10}$$

where ρ_c represents the molar density of the particle and remains constant during the interaction, since there is no ash formation, and R_0 is the initial radius of the soot particle.

The calculation of the reaction order of the interaction of Printex-U with NO was carried out on the basis of Equation 10. This equation was linearized, obtaining Equation 11, which allows the calculation of the reaction order for Printex-U interaction with respect to NO at constant temperature.

$$log\left(\frac{1}{\tau b}\right) = log\left(\frac{k_S}{\rho_C R_0}\right) + n \cdot log\, C_{NO} \tag{11}$$

The values of *b* and τ used for the determination of reaction order with respect to NO are shown in Table 4 (Experiments 1 to 5). The experimental data exhibit a relatively good fitting to Equation 11 as may be observed in Figure 6. The reaction order with respect to NO, calculated from the slope of the fitting line, is 0.26. This fractional order is in agreement with other reaction orders found in literature for different carbonaceous materials (see Table 1). Moreover, the reaction order lower than unity was expected since the NO conversion dependence on the inlet NO concentration is indicative of a fractional order lower than one. Otherwise, if NO conversion was not dependent of the inlet NO concentration, it would mean that reaction order should be around unity [18,23]. The results obtained demonstrate that the

kinetic model SCM with decreasing size particle and chemical reaction control is a good model for describing the behavior of Printex-U for its interaction with NO.

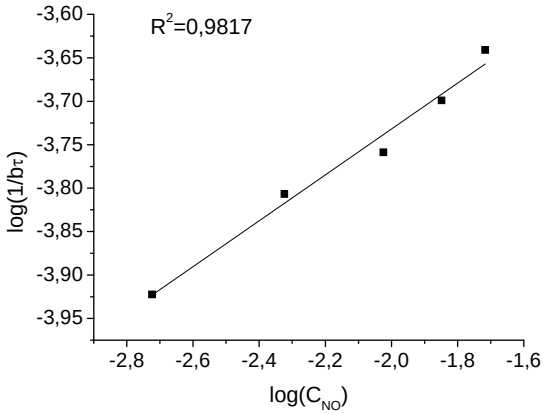

Figure 6. Determination of reaction order with respect to NO of Printex-U, according Equation 11, with different NO inlet concentrations at 1273 K.

The results obtained at different temperatures (ranging from 1173 to 1373K) allow setting the activation energy (*Ea*) for the process by means of the Arrhenius equation. The values of *b* and τ used for calculating the activation energy are shown in Table 4 (Experiments 6 to 10). Using Equation 10 and considering the reaction order of 0.26, the ($k_S/\rho_C \cdot R_0$) values were obtained at each temperature and treated by the linearized Arrhenius equation. Arrhenius equation was described as function of ρ_c and R_0 and its linearization generates, hence, Equation 12:

$$ln\frac{k_s}{\rho_c \cdot R_0} = ln\frac{k_0}{\rho_c \cdot R_0} - \frac{Ea}{R_g}\frac{1000}{T} \qquad (12)$$

where R_g is the gas constant for ideal gases (J/mol K) and T is the operation temperature (K). By representing Equation 12, Ea/R_g is obtained from the slope of the fitting line, Figure 7.

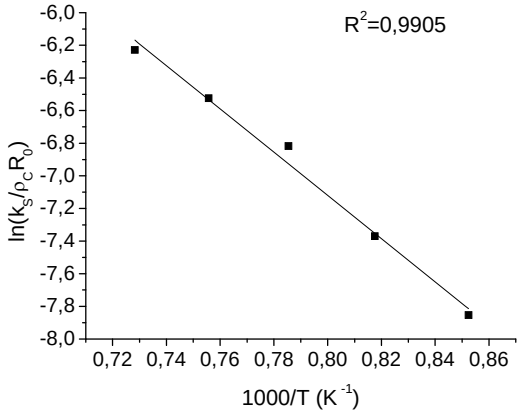

Figure 7. Arrhenius plot for Printex-U interaction with NO in the 1173-1373 K temperature range for an inlet NO concentration of 2000 ppm.

The resulting activation energy was 110 kJ/mol, which is of the order of magnitude of values obtained in literature (Table 1).

4. Conclusions

An experimental and kinetic study at high temperatures was made of the interaction of NO with Printex-U, a commercial carbon black, considered as diesel soot model compound. The experiments carried out took into account the inlet NO concentration influence (from 200 to 2000 ppm) at a given temperature of 1273 K and temperature influence (from 1173 to 1373 K) at a given inlet NO concentration of 2000 ppm.

Firstly, a characterization of the carbonaceous material was performed. From these results it was concluded that Printex-U is mainly composed by carbon, its specific area is around 90 m^2/g and the average size of the particles ranges from 30 to 45 nm.

From the experiments developed at 1273 K varying the inlet NO concentration it was observed that the more NO concentration the higher carbon conversion while NO conversion increased when the inlet NO concentration decreased.

From the experiments performed at different temperatures with an inlet NO concentration of 2000 ppm, the same trend was obtained for both conversions: the more temperature, the more carbon and NO conversion.

The kinetic model, the Shrinking Core Model with decreasing size particle and chemical reaction control, was successfully applied. From the experiments carried out with different inlet NO concentrations a fractional reaction order equal to 0.26 was obtained. The reaction order lower than unity was expected owing to the NO conversion dependence on the inlet NO concentration. From the experiments performed varying temperature, the resulting activation energy was 110 kJ/mol.

Acknowledgements

The authors express their gratitude to the MICINN (Project CTQ2009-12205) and Aragón Government-La Caixa (Project GA-LC031/2009) for financial support. Ms. C. Arnal acknowledges the Spanish Ministry of Education for the predoctoral grant awarded (AP2008-03449) and Evonik Degussa GmbH for the Printex-U supplied.

References

[1] Aarna, I., Suuberg, E.M., "A review of the kinetics of the nitric oxide carbon reaction", *Fuel* 76(6): 475-491 (1997).

[2] Xi, J., Zhong, B.J., "Soot in diesel combustion systems", *Chem. Eng. Technol.* 29(6): 665-673 (2006).

[3] Jung, J., Lee, J.H., Song, S., Chun, K.M., "Measurement of soot oxidation with NO_2-O_2-H_2O in a flow reactor simulating diesel engine DPF", *Int. J. Automot. Technol.* 9(4): 423-428 (2008).

[4] Atribak, I., Bueno-López, A., García-García, A., "Uncatalysed and catalysed soot combustion under $NO_x + O_2$: Real diesel versus model soots", *Combust. Flame* 157(11): 2086-2094 (2010).

[5] Guerrero, M., Millera, A., Alzueta, M.U., Bilbao, R., "Experimental and kinetic study at high temperatures of the NO reduction over eucalyptus char produced at different heating rates", *Energy Fuels*,. 25(3): 1024–1033 (2011).

[6] Mendiara, T., Alzueta, M.U., Millera, A., Bilbao, R., "Influence of the NO concentration and the presence of oxygen in the acetylene soot reaction with NO", *Energy Fuels*, 22(1): 284-290 (2008).

[7] Xie, G.G., Fan, W.D., Song, Z.L., Lu, H., Yu, J., Zhang, M.C., "Experimental study on soot combustion and its noncatalyzed reaction with NO", *Energy Fuels* 21: 3134-3143 (2007).
[8] Li, Y.H., Lu, G.Q., Rudolph, V., "The kinetics of NO and N_2O reduction over coal chars in fluidised-bed combustion", *Chem. Eng. Sci.* 53(1): 1-26 (1998).
[9] Suuberg, E.M., Teng, H., Calo, J.M., "Studies on the kinetics and mechanism of the reaction of NO with carbon", *Symposium (International) on Combustion* 23(1): 1199-1205 (1991).
[10] Chan, L.K., Sarofim, A.F., Beér, J.M., "Kinetics of the NO-carbon reaction at fluidized bed combustor conditions", *Combust. Flame* 52: 37-45 (1983).
[11] Aarna, I., Suuberg, E.M., "A review of the kinetics of the nitric oxide carbon reaction", *Fuel* 76(6): 475-491 (1997).
[12] Rodriguez-Mirasol, J., Ooms, A.C., Pels, J.R., Kapteijn, F., Moulijn, J.A., "NO and N_2O decomposition over coal char at fluidized-bed combustion conditions", *Combust. Flame* 99(3-4): 499-507 (1994).
[13] Kegl, B., "Influence of biodiesel on engine combustion and emission characteristics", *Applied Energy* 88(5): 1803-1812 (2011).
[14] Neeft, J.P.A., Nijhuis, T.X., Smakman, E., Makkee, M., Moulijn, J.A., "Kinetics of the oxidation of diesel soot", *Fuel* 76(12): 1129-1136 (1997).
[15] Ahlström, A.F., Odenbrand, C.U.I., "Combustion characteristics of soot deposits from diesel engines", *Carbon* 27(3): 475-483 (1989).
[16] Evonik Industries brochure.
[17] Guerrero, A., Ruiz, M.P., Alzueta, M.U., Bilbao, R., Millera, A., "Pyrolysis of eucalyptus at different heating rates: studies of char characterization and oxidative reactivity", *J. Anal. Appl. Pyrolysis* 74(1-2): 307-314 (2005).
[18] Dong, L., Gao, S., Song, W., Xu, G., "Experimental study of NO reduction over biomass char." *Fuel Process. Technol.* 88(7): 707-715 (2007).
[19] Guerrero, M., Ruiz, M.P., Millera, A., Alzueta, M.U., Bilbao, R. "Characterization of biomass chars formed under different devolatilization conditions: differences between rice husk and eucalyptus", *Energy Fuels* 22(2): 1275-1284 (2008).
[20] Arnal, C., Esarte, C., Abián, M., Millera, A., Bilbao, R., Alzueta, M.U., "Characterization and reactivity of soots obtained under different combustion conditions", *Chem. Eng. Trans*. 22: 251-256 (2010).
[21] Mendiara, T., Alzueta, M.U., Millera, A., Bilbao, R., "Oxidation of acetylene soot: Influence of oxygen concentration", *Energy Fuels* 21(6): 3208-3215 (2007).
[22] Yang, J., Sanchez-Cortezon, E., Pfander, N., Wild, U., Mestl, G., Find, J., Schlogl, R., "Reaction of NO with carbonaceous materials: III. Influence of the structure of the materials", *Carbon* 38(14): 2029-2039 (2000).
[23] Sørensen, C.O., Johnsson, J.E., Jensen, A., "Reduction of NO over wheat straw char", *Energy Fuels* 15(6) 1359-1368 (2001).
[24] Szequely, J., Evans, J.W., Sohn, H.Y., *Gas-Solid Reactions*, Academic Press: New York, 1976, p. 66.
[25] Levenspiel,O., *Chemical Reaction Engineering*, John Wiley & Sons Inc., 1999, p. 566.